Journal of Solid State Chemistry **167,** 354–362 (2002)
doi:10.1006/jssc.2001.9541

Thermoset Epoxy–Clay Nanocomposites: The Dual Role of α,ω-Diamines as Clay Surface Modifiers and Polymer Curing Agents

Costas S. Triantafillidis, Peter C. LeBaron, and Thomas J. Pinnavaia[1]

Department of Chemistry, Michigan State University, East Lansing, Michigan 48824

Received January 10, 2002; in revised form January 29, 2002; accepted February 8, 2002; published online March 27, 2002

IN HONOR OF PROFESSOR GALEN STUCKY ON THE OCCASION OF HIS 65TH BIRTHDAY

Diprotonated forms of polyoxypropylene diamines of the type α,ω-$[NH_3CHCH_3CH_2(OCH_2CHCH_3)_xNH_3]^{2+}$ with $x = 2.6$, 5.6, and 33.1, have been intercalated into montmorillonite and fluorohectorite clays and subsequently evaluated for the formation of glassy epoxy–clay nanocomposites. The intercalated onium ions functioned concomitantly as a clay surface modifier, intragallery polymerization catalyst, and curing agent. Depending on the chain length of the diamine, different orientations of the propylene oxide chains were adopted in the clay galleries, resulting in basal spacings from ~ 14 Å (lateral monolayer, $x = 2.6$) to ~ 45 Å (folded structure, $x = 33.1$). The initial clay basal spacings were correlated with the formation of intercalated and exfoliated clay–epoxy nanocomposites with improved mechanical properties and high thermal stabilities. In comparison to clay–monoamine intercalates, the use of diamine intercalates greatly reduced the plasticizing effect of the alkyl chains on the polymer matrix, resulting in improved mechanical properties while at the same time reducing the cost and time needed for nanocomposite fabrication.

INTRODUCTION

Polymer–layered silicate nanocomposites (PLSN) represent a relatively new class of organic–inorganic hybrid materials of interest for fundamental materials research studies, as well as commercial application (1–7). The PLSN materials exhibit improved physical and performance properties in comparison to pristine polymers and conventional composites, due mainly to their unique phase morphology and the interfacial properties provided by the highly dispersed silicate nanolayers in the polymer matrix. These effects are minimized for conventional composites, where the inorganic additives have dimensions in the macroscopic (μm) length scale. Consequently improved properties can be achieved at a considerably lower concentration of the inorganic phase for PLSN materials in comparison to conventional composites. Loadings of only ~ 5 wt% exfoliated silicate nanoparticles in PLSN materials result in significant enhancement in mechanical properties (modulus, strength, thermal expansion coefficient), barrier properties, thermal stability, resistance to solvent swelling, flammability resistance and ablation performance.

A wide variety of layered materials are potentially well suited for the formation of organic–inorganic nanocomposites because their lamellar elements have high in-plane strength and stiffness and a high aspect ratio. However, the smectite clays (8) (e.g., montmorillonite, hectorite) and related layered silicates are the materials of choice for polymer nanocomposites design, mainly because of their rich intercalation chemistry which allows them to be chemically modified and to become compatible with the polymer precursors. Additionally, they occur ubiquitously in nature and can be purified at relatively low cost.

An organo montmorillonite clay way first exfoliated into a thermoplastic nylon-6 polymer, resulting in a commercialized product with enhanced thermo-mechanical properties. The organo clay was synthesized by ion-exchanging the cations of the parent clay with more hydrophobic organic onium ions (9–11). Subsequent research focused on issues relating to the most suitable organic modifier of the clay and the best conditions for the formation of the exfoliated nanocomposites. Nanocomposites formed with thermoset polymers, especially epoxy resins, and modified smectite clays (12–25) and other layered silicates, such as layered silicic acids (e.g., magadiite) (26), also have received considerable attention. It has been previously shown that acidic primary onium ions, when they are ion-exchanged for the inorganic cations of the parent layered silicates, catalyze the intragallery epoxide polymerization process in the presence of diamine curing agent (21, 26). The chain length of the onium ion, its relative acid strength (primary > second-

[1] To whom correspondence should be addressed. Fax: + 517-432-1225. E-mail: pinnavai@cem.msu.edu.

0022-4596/02 $35.00

ary > tertiary onium ions) and the clay layer charge density, which dictates the concentration of the organic modifier in the galleries, all play an important role in clay nanolayer exfoliation. In general, the catalytic activity of the acidic onium ions is more pronounced when the alkyl chains of the onium ions provide an intragallery hydrophobic environment that is compatible with both the epoxy polymer precursors and the diamine curing agent. More recently (17), it was shown that the use of a hydroxyl-substituted quaternary ammonium modifier in a montmorillonite clay resulted in a high degree of clay layer exfoliation, quite similar to the activity of the acidic onium ions.

In an effort to optimize the overall process of the formation of thermoset epoxy–clay nanocomposites, we have focused here on the synthesis of a new type of potentially advantageous organo smectite clays. The direct incorporation of the primary diamine curing agents in the galleries of montmorillonite and fluorohectorite clays in the form of diprotonated diamines by an ion-exchange process is presented as an alternative, less process intensive way of preparing epoxy–clay nanocomposites. Different degrees of clay nanolayer intercalation/exfoliation could be achieved, depending mainly on the chain length and the concentration of the diamine in the gallery. An appreciable improvement in the mechanical properties could be found for all the nanocomposite compositions formed.

EXPERIMENTAL SECTION

Materials

The epoxide resin used for the formation of the pristine glassy epoxy polymer and the epoxy–clay nanocomposites was a diglycidyl ether of bisphenol A (DGEBA), more specifically, Shell EPON 826 with MW ~ 369 and epoxy equivalent weight ~182:

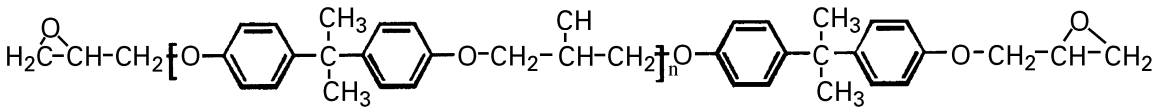

$n = 0$ (90%), 1 (10%).

The curing agent was polyoxypropylene diamine, provided under the trade name Jeffamine D230 by Huntsman Chemicals with the following structural formula:

$$NH_2CHCH_3CH_2(OCH_2CHCH_3)_xNH_2$$

and a molecular weight of ~230 ($x = 2.6$).

Jeffamines D2000 (MW ~ 2000, $x = 33.1$), D400 (MW ~ 400, $x = 5.6$) and D230 (MW ~ 230, $x = 2.6$) were used for the preparation of the organo clays, as is described below. All other chemicals used in this work were purchased from Aldrich Chemical Co. and used without further purification.

Inorganic and Organic Clays

An industrially purified Na^+-montmorillonite (PGW, Nanocor Inc.) with a cation exchange capacity (CEC) of 120 meq/100 g, was converted to the H^+- and Li^+-exchanged forms by ion-exchange with dilute HCl or LiCl aqueous solutions, respectively. A synthetic Li^+-fluorohectorite clay (FH, Corning Inc.) with a CEC similar to that of the PGW montmorillonite was used as the parent fluorohectorite clay in this study.

The organic clays were prepared by ion-exchanging the inorganic clay with the diprotonated forms of Jeffamine diamines D2000, D400, and D230. Stoichiometric amounts of the diamine and dilute aqueous HCl in small excess of the ion-exchange capacity of the clay were used to ensure the formation of the diprotonated diamines. The acidic Jeffamine solution was then blended with an aqueous suspension of the inorganic clay for 1–2 min. The blended mixture was further stirred for 48 h at ambient temperature. In the case of D230, a second sample was prepared by ion-exchanging the parent clay using double the stoichiometric amount of diamine, in order to achieve higher degree of ion-exchange. The ion-exchanged clays were separated by centrifugation, washed 3–4 times with deionized water (until free of Cl^-) and once with EtOH, prior to air-drying at room temperature. The dried products were ground and sieved to a particle size < 270 mesh (53 μm). Table 1 provides the compositions and basal spacings for the clays used for nanocomposite formation.

Polymer and Polymer Nanocomposite Formation

The pristine glassy epoxy polymer was formed by mixing the epoxy monomer (EPON 826) with the curing agent (Jeffamine D230) at 50° C for ~30 min, outgassing of the liquid mixture at room temperature and curing in the RTV silicone rubber molds at 75° C for 3 h, then at 125° C for an additional 3 h under nitrogen.

The preparation of epoxy–clay nanocomposites was similar to the pristine polymer formation. The clay was added to the epoxy EPON 826 – curing agent D230 mixture at 50° C under stirring for 30 min. The mixture was outgassed and cured at 75° C for 3 h, then at 125° C for 3 h (procedure *P*-1). Alternatively, the epoxy EPON 826 was initially mixed with the clay at 50°C and then the D230 curing agent was added (procedure *P*-2). In the case of the organic clays intercalated by Jeffamine D2000, D400, and D230, the moles of onium ions present in the organic clay were counted as contributing to curing process. That is, the intercalated

TABLE 1
Compositions and Basal Spacings of the Montmorillonite (PGW) and Fluorohectorite (FH) Clays Used for the Preparation of Epoxy Nanocomposites

		Organic modifier[a]		Basal spacings	
Intercalated clay	Parent clay	Diprotonated diamine	Onium ion exchange[b] (%)	d_{001} (Å)	d_{002} (Å)
H-PGW	Na-PGW	—	—	13.4	—
Li-PGW	Na-PGW	—	—	12.4	—
Li-FH	Li-FH	—	—	12.3	—
D2000-PGW	Na-PGW	D2000	80	45.5	21.8
D400-PGW	Na-PGW	D400	90	17.2	—
D230-PGW	Na-PGW	D230	85	13.8	—
D230/high-PGW[c]	Na-PGW	D230	95	13.8	—
D2000-FH	Li-FH	D2000	80	46.0	23.1
D400-FH	Li-FH	D400	85	17.2	—
D230-FH	Li-FH	D230	80	13.8	—
D230/high-FH[c]	Li-FH	D230	95	14.0	—

[a] The inorganic clays were ion-exchanged with diprotonated Jeffamine diamines of the type $[NH_3CHCH_3CH_2(OCH_2CHCH_3)_xNH_3]^{2+}$, denoted as D230 ($x = 2.6$), D400 ($x = 5.6$), and D2000 ($x = 33.1$).

[b] The percent onium ion-exchange represents the extent to which the ion-exchange sites of the clay have been replaced by onium ions; the reported values were determined by TGA analysis.

[c] The amount of D230 used for the ion-exchange of this sample was twice the amount necessary for stoichiometric exchange of Na^+ or Li^+ ions with onium ions.

diamine was supplementary to the amine groups of Jeffamine D230, which was the main curing agent for the formation of the glassy epoxy polymers. The amount of onium ions used as the organic clays modifier was always $< 4\%$ of the total amine groups needed for the complete cross-linking of the epoxy monomers. The clay loadings for the nanocomposites were 1.0, 3.0 and 6 wt% on a silicate basis.

Characterization and Testing

X-ray diffraction (XRD) patterns were obtained on a Rigaku rotaflex 200B diffractometer equipped with Cu$K\alpha$ X-ray radiation and a curved crystal graphite monochromator, operating at 45 kV and 100 mA. The diffraction patterns were collected between 1 and 12° at a scanning rate of 1°/min. Samples of the liquid (gel-like) epoxy–clay mixtures or of the uncured epoxy—curing agent–clay mixtures were prepared by applying a thin film on filter paper mounted on a glass slide. Cured composite samples were prepared by mounting a rectangular flat specimen into an aluminum holder.

Transmission electron microscopy (TEM) images were obtained on a JEOL JEM-100CX II microscope with a CeB_6 filament and an accelerating voltage of 120 kV, a beam diameter of ~ 5 μm and an objective aperture of 20 μm. The TEM samples were prepared by supporting thin sections (80–100 nm) of the nanocomposite samples onto 300 mesh nickel grids.

Dynamic mechanical analysis (DMA) tests were performed on a 2980 Dynamic Mechanic Analyzer (TA instruments) in the three-point bending mode at a frequency of 1 Hz and amplitude of 20 μm over the temperature range 25–140° C. The heating rate was 4° C/min. The pristine epoxy polymer and the nanocomposite specimens were rectangular bars with dimensions 60 mm × 13 mm × 3 mm.

Thermogravimetric analyses (TGA) were performed using a Cahn TG System 121 Analyzer. The powdered clays, the pristine epoxy polymer, and the nanocomposite samples were heated to 800° C at a rate of 5° C/min under N_2 flow.

The compositions of the inorganic and organic clays were determined by energy dispersive spectroscopy (EDS), CHN chemical analysis and TGA analysis.

RESULTS AND DISCUSSION

Synthesis of Diamine Clay Intercalates

The intercalation of onium ions in layered silicate by ion-exchange procedures results in different spacing between the silicate nanolayers due to the different potential configurations of the organic modifier (27, 28). Ordinarily, when simple alkylammonium ions with a C_{12}–C_{18} carbon chain are ion-exchanged for the inorganic cations in smectite clays with a CEC $\sim$ 100–120 meq/100 g, they adopt a lateral bilayer ($\sim$18 Å) or an inclined paraffin-like structure ($\sim$20–23 Å). A pseudo-trilayer or a lipid-like bilayer configuration at higher onium ion concentrations are also possible (4, 29). However, at relatively high concentrations of the alkylammonium ions, the formation of undesirable dangling alkyl chains resulting from the excess of the onium ions in the gallery relative to the stoichiometric cross-linking of the epoxy groups, will have a negative effect on the nanocomposite's properties, especially when quaternary alkylammonium ions are used (26).

The utilization of diprotonated Jeffamine diamines of the type $[NH_3CHCH_3CH_2(OCH_2CHCH_3)_xNH_3]^{2+}$ as the organic modifier of the clay eliminates the undesirable effect of alkyl dangling chains. The XRD patterns of fluorohectorite (FH) intercalated by the diprotonated Jeffamines D230 ($x = 2.6$), D400 ($x = 5.6$), and D2000 ($x = 33.1$) are shown in Fig. 1. Similar patterns were obtained for the corresponding PGW montmorillonite intercalates. The spacings for the d_{001} basal reflection indicate that the short chain, low MW Jeffamine D230 ($x = 2.6$) adopts a lateral monolayer structure (13.8 Å). For the longer chain Jeffamine D400 ($x = 5.6$), the basal spacing of D400-FH at $\sim$85% ion-exchange was $\sim$17.5 Å, consistent with a lateral bilayer or an inclined layer-to-layer configuration of the diprotonated diamine molecules, similar to the case of C_{12}–C_{18} alkylammonium ions. On the other hand, ion-

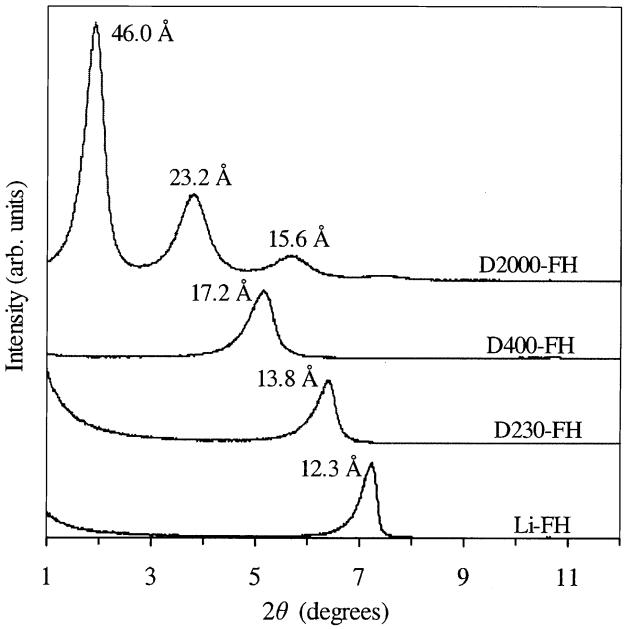

FIG. 1. X-ray diffraction patterns of the fluorohectorite (FH) intercalated by diprotonated Jeffamine onium ions of the type $[NH_3CHCH_3CH_2(OCH_2CHCH_3)_xNH_3]^{2+}$ and denoted D230 ($x = 2.6$), D400 ($x = 5.6$) and D2000 ($x = 33.1$).

exchange of the parent clay with the diprotonated Jeffamine D2000 ($x = 33.1$) resulted in a *d*-spacing of ~ 46 Å, indicative of a structure where the long propylene oxide chains adopt a folded configuration. The structures of the homoionic Jeffamine-intercalated clays are schematically represented in Fig. 2. The compositions and X-ray basal spacings for the intercalates are given in Table 1.

Epoxy–Clay Nanocomposite Formation from Jeffamine Diamine Clay Intercalates

The complexity of a three-component system (resin, curing agent, organo clay) for the preparation of a thermoset epoxy–clay nanocomposite is very well described in the recent work by Vaia *et al.* (17). The preferred sequence of component mixing (organo clay/curing agent/epoxy), the use of solvents to reduce the viscosity of the system, the temperature and time of curing, and finally the fabrication techniques could have a significant effect on the quality of the final nanocomposite material. With regard to the preparation of the reaction mixture before curing, the compatibility of the organic modifier with both the epoxy monomers and the curing agent should be considered. In the case of the diprotonated diamine intercalates used in this study, it appears that the conditions are optimum for dissolving the epoxy monomers in the clay galleries and for initiating epoxide polymerization through acid catalysis. However, in order to avoid gelling the system prematurely, care was taken in pre-mixing the diamine-modified organic clay with the epoxy monomers. In general, the mixing temperature was below 50° C and the mixing time was < 24 h. Efficient mixing of the epoxide and organo clay could also be achieved through the use of low-boiling-point solvents for reducing the viscosity and facilitating the insertion of the epoxy monomers in the galleries.

The formation of an epoxy–exfoliated clay nanocomposite requires the polymer precursors to polymerize inside the clay galleries at a rate competitive with the polymerization rate outside the galleries. This was clearly the case for both the D2000-PGW and the D2000-FH organic clays. Figure 3 shows the XRD patterns of D2000-FH clay in which the epoxy monomer was progressively intercalated resulting in *d*-spacing values of ~ 59 Å after 6 h reaction (Fig. 3a) and ~ 64 Å after 24 h reaction (Fig. 3b) at 50° C. After the addition of the D230 curing agent (the short chain diamine D230 needed for the formation of the rigid epoxy polymer), a very broad peak/shoulder with *d*-spacing of ~ 30 Å dominated the XRD pattern. The peak became broader and weaker after heating the mixture at 75° C for 30 min, as shown in Fig. 3c. The XRD pattern of the final, cured nanocomposite (6 wt% silicate loading) is shown in Fig. 3d. The in-plane structural integrity of the clay in the nanocomposite was verified by the presence of the 060 reflection in the XRD pattern of the exfoliated clay nanocomposite (inset in Fig. 3d).

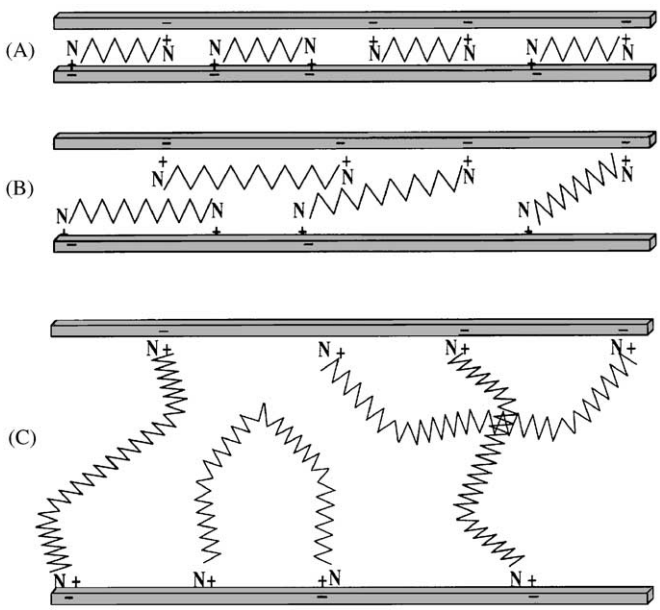

FIG. 2. Schematic representation of the orientations of the diprotonated Jeffamine onium ions intercalated in the galleries of a homoionic organo smectite clay: (a) D230 lateral monolayer (13.8 Å); (b) D400 lateral bilayer to inclined monolayer (17.2 Å); (c) D2000 folded chain structure (~ 46 Å).

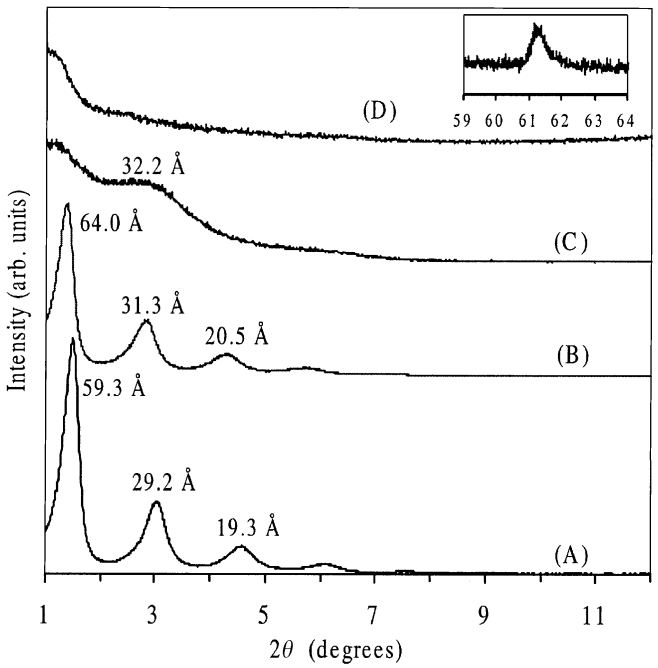

FIG. 3. X-ray diffraction patterns of mixtures of D2000-FH clay, EPON 826 epoxy monomer and Jeffamine D230 curing agent: (a) after intercalation of EPON 826 in D2000–FH at 50° C for 6 h; (b) after intercalation of EPON 826 for 24 h; (c) after addition of D230 in the mixture of step b, outgassing and heating at 75° C for 0.5 h; (d) after curing 3.0 h at 75° C and 3.0 h at 125° C. The clay loading was 6 wt% on a silicate basis for patterns c and d. The inset shows the presence of an in-plane 060 clay reflection in the cured nanocomposite.

It is noteworthy that pre-intercalation of the epoxy monomer in the D2000-FH organo fluorohectorite did not alter the lamellar ordering of the clay, although the *d*-spacing increased by $\sim$20 Å to a relatively high value of $\sim$65 Å in comparison to the swelling observed previously for other organo layered silicates by epoxy resins (17, 26). The retention of a layered stacking order over such a high degree of gallery swelling may result in part from electrostatic interactions between the onium ions of the α,ω-diamine in a paraffin-like arrangement and the negatively charged clay layers. Such interactions would link adjacent layers even in the presence of a high degree of swelling and thereby retain the stacking integrity of the nanolayer tactoids. In the case of the D2000-PGW organo montmorillonite clay, the degree of lamellar ordering was lowered upon swelling with the epoxy monomers, since both the (001) and (002) reflections in the XRD pattern (not shown) were relatively broad compared to those in the XRD pattern of D2000-FH fluorohectorite (see Figs. 3a and 3b). The lower aspect ratio of PGW montmorillonite ($\sim$200) compared to FH fluorohectorite ($\sim$2000) may contribute to the higher tendency for montmorillonite to lose its layer stacking order more easily during pre-intercalation by the epoxy monomers. Nevertheless, for both types of clays, the basal spacings of the epoxy–swollen clay intercalates are high enough to ensure clay nanolayer exfoliation upon curing with the D230 diamine.

The above nanolayer intercalation/exfoliation behavior is in accord with the findings from the TEM images of the nanocomposites prepared form D2000-FH (Figs. 4a and 4b) and D2000-PGW (Figs. 4c and 4d), at clay loading of 6 wt% (silicate basis). The D2000-FH fluorohectorite nanocomposite consisted mainly of tactoids with disordered, highly intercalated layers of high aspect ratio ($\geq$ 1000 nm), with basal spacing between 5 and 15 nm. Individual, shorter layers could also be found on the edges of the primary dispersed particles and most frequently in domains with relatively low number of layers. On the other hand, the nanolayers of the D2000-PGW montmorillonite clay with a lower layer aspect ratio were more randomly dispersed in the polymer matrix and were highly intercalated or partially exfoliated.

The XRD patterns of the nanocomposites formed from the inorganic proton-exchanged PGW clay, and of those prepared from the D230, D400, and D2000 exchanged PGW montmorillonite clays are shown in Fig. 5. The XRD patterns of the samples prepared with the D230 and D400 exchanged clays showed that no significant intercalation occurred during the polymerization process (Figs. 5b and 5c, respectively). This behavior could be easily explained for D230-PGW or D230-FH clay intercalates due to the very short carbon chain of the D230 diamine and the correspondingly small gallery heights that limit swelling. Also, there was no improvement in swelling when the highly exchanged D230-clay was tested for the formation of nanocomposites. However, in the case of D400, the *d*-spacing of both the D400-FH and D400-PGW organo clays was $\sim$17.2 Å, similar to that of a primary C_{18}-alkylammonium exchanged montmorillonite clay, which also was tested in the present work for comparison purposes. The degree of clay nanolayer intercalation was significantly higher with the C_{18}-montmorillonite compared to the D400-clays, although both organo clays had similar *d*-spacing values. This behavior could be attributed to the above-suggested mechanism where the electrostatic interactions between the two onium ions of the diamines and the clay layers are strong enough to inhibit any significant intercalation. Interestingly, the composite samples prepared by the D230-PGW and the D400-PGW clays exhibited very good mechanical properties (see below). Furthermore, the 3-mm-thick specimens, which were prepared for DMA tests, were optically transparent.

In contrast to the non-intercalated composite samples formed from D230- and D400-exchanged clays, the use of the inorganic H^+- and Li^+-clays resulted in samples where nearly 20 wt% of the added clay (6 wt% silicate) settled at the bottom of the composite specimen. However, the nanolayers of a D2000-clay intercalate could be exfoliated

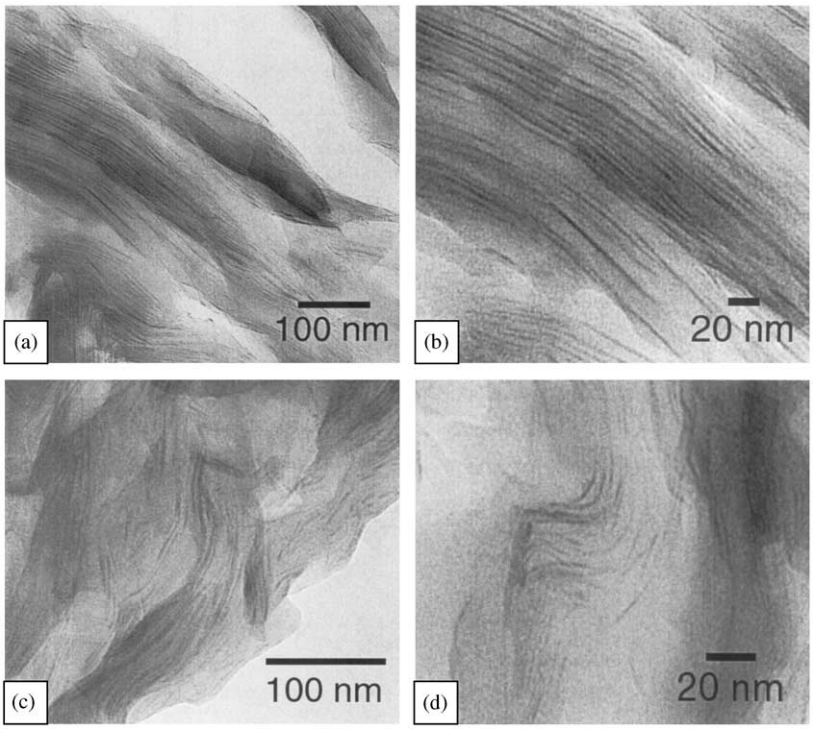

FIG. 4. TEM images of thin sections of the glassy epoxy nanocomposites prepared from EPON 826 resin and D230 curing agent in the presence of organo clays (a, b) D2000–FH fluorohectorite clay and (c, d) D2000–PGW montmorillonite clay. The clay loading of the nanocomposite samples was 6.0 wt% on a silicate basis.

in a glassy epoxy matrix by pre-intercalating the diamine in a H^+-exchanged clay before the addition of the epoxy resin. In this way, the time-consuming step of synthesizing the organic clay could be eliminated since an *in situ* organo clay synthesis can be accomplished by using a H^+-clay that is otherwise incapable of forming an exfoliated nanocomposite.

Properties of the Nanocomposites

The effect of clay nanolayer reinforecement on the mechanical properties of the glassy epoxy polymer were investigated by dynamic mechanic analysis (DMA). In the DMA technique an oscillatory force is applied to a sample and the response to that force is analyzed (30). Two different moduli are determined as a function of temperature, an elastic or storage modulus (E'), which is related to the ability of the material to return or store energy, and an imaginary or loss modulus (E''), which relates the ability of the polymer to disperse energy. The temperature dependence of the ratio E''/E', also called tan delta (tan δ), is related to the mechanical properties of the (nano)composites. The maximum in a tan δ vs temperature plot may be taken as an estimate of the glass transition temperature (T_g). Care needs to be taken when comparing DMA results from previously reported studies, because different DMA modes, such flexural and torsional modes, can be applied to the sample. The curves in Fig. 6a and 6b show the dependence of the storage modulus and tan δ on temperature, as determined by the three-point bending (flexural) DMA method. The data in Table 2 provide the storage modulus values of the pristine polymer and the nanocomposite samples at 40° C (i.e., the glassy region below tan δ_{max}) and at 110° C (i.e., the rubbery region above tan δ_{max}). The T_g values of the samples as determined from tan δ_{max} are also provided in the table.

The storage modulus in both the glassy and rubbery regions is higher for the nanocomposite samples prepared from the diamine-exchanged organic clays (6 wt% silicate loading) in comparison to the pristine epoxy polymer. Even the polymer filled by un-exfoliated H^+- and Li^+-clays exhibited improved stiffness. For the nanocomposite containing D2000-PGW montmorillonite, a 25% increase in storage modulus was observed in both regions. The composite samples formed from the D230-PGW and D400-PGW clays showed a similar increase of the storage modulus, although the clays in these samples were not exfoliated (XRD data). Increases of 35% (glassy region) and 65% (rubbery region) in storage modulus were observed for the D2000-FH nanocomposite sample, while the increase was even higher for the non-intercalated D230- and 400-FH composite samples (e.g., 35% in the glassy region and 75–150% in the rubbery region). The advantage of the

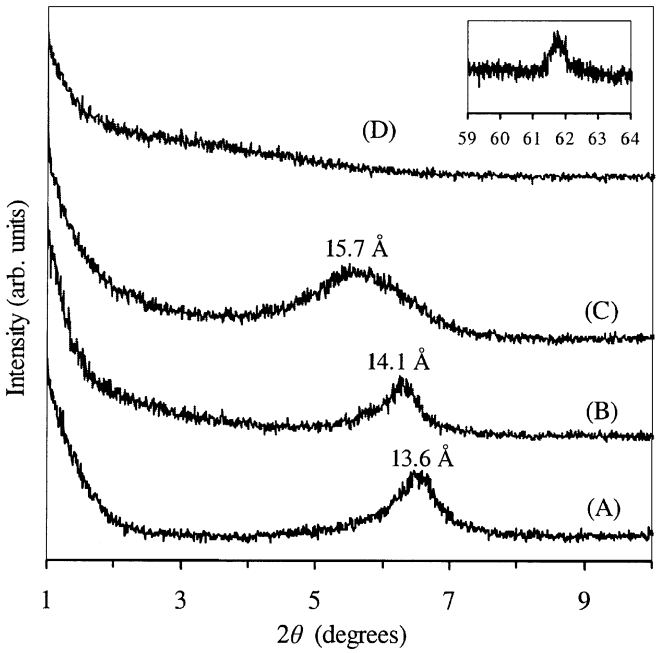

FIG. 5. X-ray diffraction patterns of EPON 826–Jeffamine D230 PGW nanocomposites formed from the following clays: (a) H^+-PGW, (b) D230-PGW, (c) D400-PGW and (d) D2000-PGW montmorillonites. The clay loading of each nanocomposite sample was 6 wt% on a silicate basis. The inset shows the presence of an in-plane 060 clay reflection in the cured nanocomposite.

higher aspect ratio of the organo fluorohectorite clays compared to the montmorillonite clays is clearly manifested in the higher moduli for the fluorohectorite nanocomposites. The observed increase in storage modulus is similar to the increases found in previous related studies (17, 24, 25), but it should be mentioned that the absolute modulus values observed by the DMA technique for the pristine epoxy polymer of the present work (e.g., $\sim$3 GPa below tan δ_{max} and $\sim$18 MPa above tan δ_{max}) are higher than those previously reported.

Relatively small changes in glass transition temperature (T_g) were observed for the nanocomposites in comparison to the pristine epoxy polymer. The small amount of D2000 ($<5\%$) introduced into the epoxy matrix from the onium ions of the organo clay galleries most likely has a small plasticizing effect on the matrix, as indicated by the decrease in T_g with increasing D2000-PGW montmorillonite loading (see Table 2). Evidence for a small plasticizing effect is provided by the lower T_g values for the pristine polymer formed when a similar amount of D2000 was incorporated into the D230 curing agent ($\sim$4% mol of the total curing agent). Also, the data in Table 2 show that there is an advantage to pre-mixing the organo clay with the epoxy resin before the addition of the curing agent in order to achieve better nanolayer exfoliation (procedure *P*-2). This latter procedure gave a 5°-higher T_g value in comparison to the standard procedure in which the organo clay was added directly to the epoxy–curing agent mixture (procedure *P*-1).

Thermogravimetric analyses provided additional information on the properties of both the onium ion intercalated clays and the epoxy–clay nanocomposites made from these clays. From the TGA curves in Figs. 7 and 8 and the onset temperature for thermal decomposition, which is taken as the temperatures at which the composites experienced a 1.5% loss in weight (see Table 2), we find that the

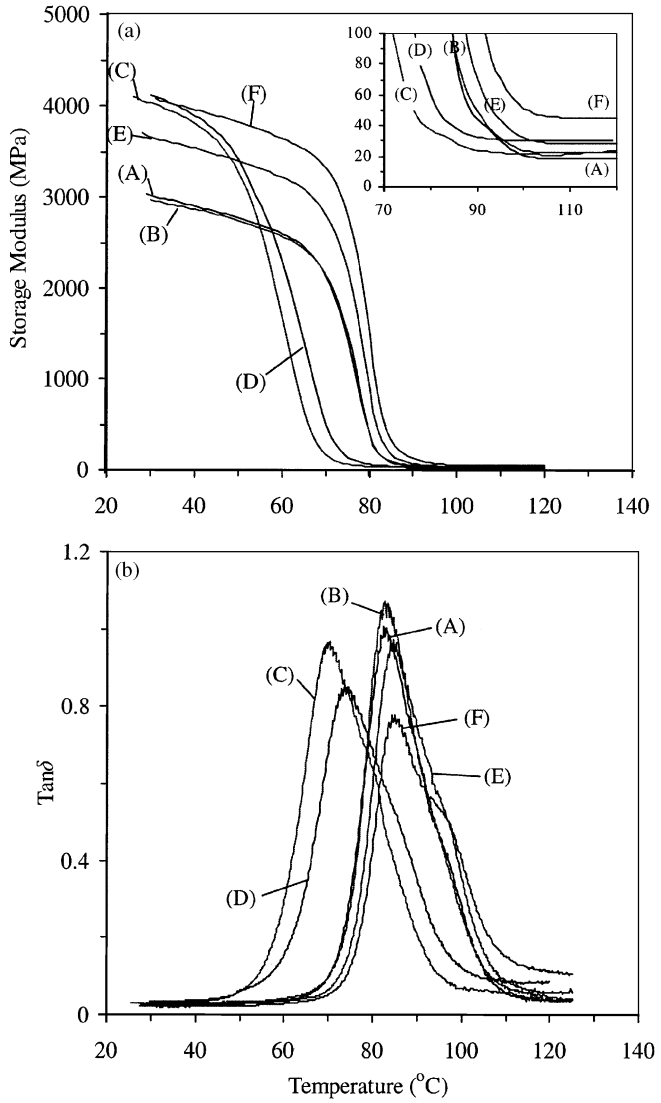

FIG. 6. Dynamic mechanical analysis measurements: (a) storage modulus vs temperature and (b) tan δ vs temperature for (A) pristine epoxy polymer prepared from EPON 826 resin and Jeffamine D230 curing agent and for the corresponding nanocomposites containing the following clays; (B) H^+-PGW, (C) D2000-PGW, (D) D2000-FH, (E) D230-PGW, (F) D230-FH. The clay loading for each nanocomposite sample was 6.0 wt% on a silicate basis.

TABLE 2
Dynamic Mechanical Analysis and Thermal Analysis Data for Pristine Epoxy Polymer and Polymer–Clay Nanocomposites[a]

Clay additive	Storage modulus (E') At 40° C GPa (±10%)	Storage modulus (E') At 110° C MPa (±10%)	T_g (tan δ_{max}) °C (± 2°)	Thermal stability[b] (TGA data) °C
Pristine epoxy-A(0% clay)	2.9	18.4	82.6	373
Pristine epoxy-B[c](0% clay)	3.0	20.1	75.5	361
H-PGW	2.9	22.1	82.8	354
Li-PGW	2.7	19.9	82.3	356
Li-FH	3.1	25.2	85.2	351
D2000-PGW (1 wt% clay)	3.5	21.5	81.2	345
D2000-PGW (3 wt% clay)	3.6	22.1	76.8	341
D2000-PGW	3.8	21.5	69.8	336
D2000-PGW[d]	3.6	24.0	75.1	339
D400-PGW	3.6	23.2	84.2	346
D230-PGW	3.5	28.3	84.5	358
D2000-FH	3.9	30.5	73.7	323
D400-FH	3.9	32.1	79.1	340
D230-FH	4.0	45.4	84.7	345

[a] The clay loading was 6.0 wt% on a silicate basis, unless otherwise stated.
[b] Temperature at which the TGA weight loss was 1.5%.
[c] Substitution of 4.0 mol% D2000 (organic clay modifier) for D230 (curing agent) in the pristine epoxy polymer.
[d] Nanocomposite sample prepared by pre-mixing of epoxy monomers with the organo clay (procedure *P*-2); the remaining nanocomposite samples were prepared by direct addition of the clay additive to the epoxy resin–curing agent mixture (procedure *P*-1).

thermal stability of the nanocomposites was not greatly compromised by the presence of the long chain D2000-organic modifier. It is quite interesting to note that Jeffamine onium ions undergo facile thermal decomposition, presumably the well-known Hofmann degradation (31), when intercalated into montmorillonite and fluorohec-

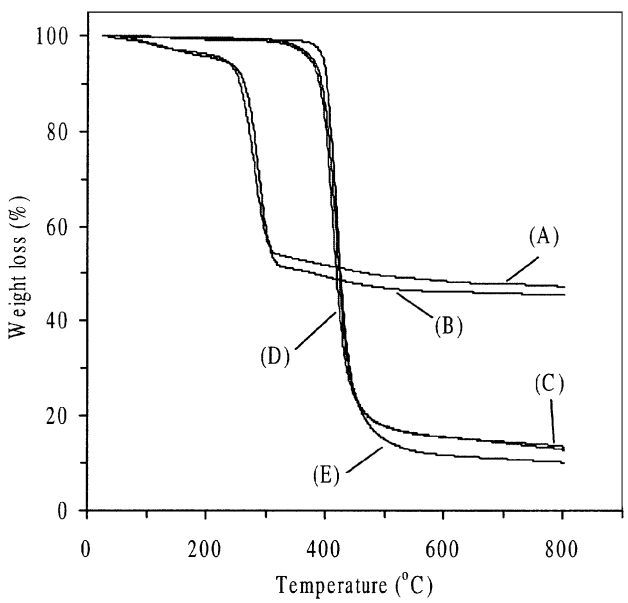

FIG. 7. TGA curves for the organo clays (a) D2000-PGW montmorillonite and (b) D2000-FH fluorohectorite and the corresponding nanocomposites prepared from (c) D2000-PGW and (d) D2000-FH clays. Curve (e) is for the pristine polymer prepared from EPON 826 resin and Jeffamine D230 curing agent. The clay loading for each nanocomposite sample was 6.0 wt% on a silicate basis.

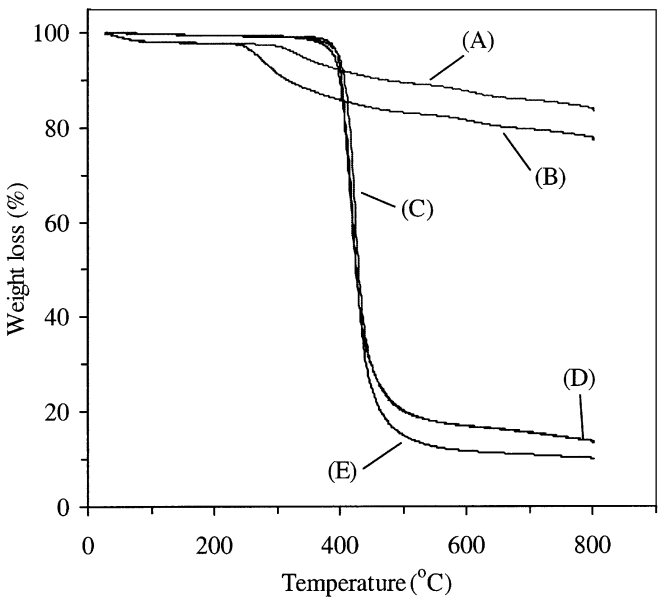

FIG. 8. TGA curves for the organo clays (a) D230-PGW montmorillonite and (b) D400-PGW montmorillonite and for the epoxy nanocomposites prepared from (c) D230-PGW and (d) D400-PGW clays. Curve (e) is for the pristine polymer prepared from EPON 826 resin and Jeffamine D230 curing agent. The clay loading for each nanocomposite sample was 6.0 wt% on a silicate basis.

torite clays, as evidenced by TGA curves a and b in Figs. 7 and 8. However, there is no indication of onium ion degradation in any of the cured polymer–clay nanocomposites, whether the clay nanolayers are exfoliated or not (see curves c and d in Figs. 7 and 8). This signifies that all of the D2000 onium ions in the exfoliated nanocomposite, as well as the D230 and D400 onium ions in the intercalated composites, react completely with the epoxy resin to form a cured epoxy matrix. This latter result is in accord with the improved mechanical properties of the composites.

ACKNOWLEDGMENTS

This work has been supported by the NASA John Glenn Research Laboratory, the MSU Center for Fundamental Materials Research, and the MSU Composite Materials and Structure Center.

REFERENCES

1. R. A. Vaia and E. P. Giannelis, *MRS Bull.* **26,** 394–401 (2001).
2. T. J. Pinnavaia and G. W. Beall, Eds., "Polymer–Clay Nanocomposites." John Wiley & Sons Ltd., New York, 2000.
3. R. A. Vaia and R. Krishnamoorti, Eds., "Polymer Nanocomposites." American Chemical Society, Washington, DC, 2001.
4. P. C. LeBaron, Z. Wang, and T. J. Pinnavaia, *Appl. Clay Sci.* **15,** 11–29 (1999).
5. E. P. Giannelis, *Adv. Mater.* **8,** 29–35 (1996).
6. A. Okada and A. Usuki, *Mater. Sci. Eng. C-Biomimet. Mater. Sens. Syst.* **3,** 109–115 (1995).
7. G. Lagaly, *Appl. Clay Sci.* **15,** 1–9 (1999).
8. T. J. Pinnavaia, *Science* **220,** 365–371 (1983).
9. A. Usuki, M. Kawasumi, Y. Kojima, A. Okada, T. Kurauchi, and O. Kamigaito, *J. Mater. Res.* **8,** 1174–1178 (1973).
10. A. Usuki, Y. Kojima, M. Kawasumi, A. Okada, Y. Fukushima, T. Kurauchi, and O. Kamigaito, *J. Mater. Res.* **8,** 1179–1184 (1993).
11. Y. Kojima, A. Usuki, M. Kawasumi, A. Okada, Y. Fukushima, T. Kurauchi, and O. Kamigaito, *J. Mater. Res*, **8,** 1185–1189 (1993).
12. A. S. Zerda and A. J. Lesser, *J. Polym. Sci. B-Polym. Phys.* **39,** 1137–1146 (2001).
13. I. J. Chin, T. Thurn-Albrecht, H. C. Kim, T. P. Russell, and J. Wang, Polymer **42,** 5947–5952 (2001).
14. X. Kornmann, H. Lindberg, and L. A. Berglund, *Polymer* **42,** 4493–4499 (2001).
15. J. K. Lu, T. C. Ke, Z. N. Qi, and X. S. Yi, *J. Polym. Sci. B-Polym. Phys.* **39,** 115–120 (2001).
16. Y. C. Ke, L. Wang, and Z. N. Qi, *Acta Polym. Sin.* **9,** 768–773 (2000).
17. J. M. Brown, D. Curliss, and R. A. Vaia, *Chem. Mater.* **12,** 3376–3384 (2000).
18. X. Kornmann, H. Lindberg, and L. A. Berglund, *Polymer* **42,** 1303–1310 (2001).
19. J. H. Kang, S. G. Lyu, and G. S. Sur, *Polym.-Korea* **24,** 571–577 (2000).
20. Y. C. Ke, J. K. Lu, X. S. Yi, J. Zhao, and Z. N. Qi, *J. Appl. Polym. Sci.* **78,** 808–815. (2000).
21. T. Lan, P. D. Kaviratna, and T. J. Pinnavaia, *Chem. Mater.* **7,** 2144–2150 (1995).
22. T. Lan and T. J. Pinnavaia, *Chem. Mater.* **6,** 2216–2219 (1994).
23. M. S. Wang and T. J. Pinnavaia, *Chem. Mater.* **6,** 468–474 (1994).
24. J. Massam and T. J. Pinnavaia, *Mater. Res. Soc. Symp. Proc.* **520,** 223–232 (1998).
25. P. B. Messersmith and E. P. Giannelis, *Chem. Mater.* **6,** 1719–1725 (1994).
26. Z. Wang and T. J. Pinnavaia, *Chem. Mater.* **10,** 1820–1826 (1998).
27. G. Lagaly, *Solid State Ion.* **22,** 43–51 (1986).
28. E. Hackett, E. Manias, and E. P. Giannelis, *J. Chem. Phys.* **108,** 7410–7415 (1998).
29. Z. Wang, J. Massam, T. J. Pinnavaia, "Polymer–Clay Nanocomposites" (T. J. Pinnavaia and G. W. Beall, Eds.), pp. 127–149. John Wiley & Sons Ltd., New York, 2000.
30. K. P. Menard, "Dynamic Mechanical Analysis: A Practical Introduction." CRC Press LLC, Boca Raton, FL, 1999.
31. T. W. G. Solomons, "Organic Chemistry, 6th edn." Chap. 20, p. 940. John Wiley & Sons, Inc., New York, 1996.